Electrically Triggered Release of a Small Molecule Drug from a Polyelectrolyte Multilayer Coating

Citation: Schmidt, Daniel J., Joshua S. Moskowitz, and Paula T. Hammond 2010Electrically Triggered Release of a Small Molecule Drug from a Polyelectrolyte Multilayer Coating. Chemistry of Materials 22(23): 6416–6425.

As Published: http://dx.doi.org/10.1021/cm102578j

Publisher: American Chemical Society

Persistent URL: http://hdl.handle.net/1721.1/79054

Version: Author's final manuscript: final author's manuscript post peer review, without publisher's formatting or copy editing

Published in final edited form as:
Chem Mater. 2010 December 14; 22(23): 6416–6425. doi:10.1021/cm102578j.

Electrically Triggered Release of a Small Molecule Drug from a Polyelectrolyte Multilayer Coating

Daniel J. Schmidt, **Joshua S. Moskowitz**, and **Paula T. Hammond***
Department of Chemical Engineering, Massachusetts Institute of Technology, 77 Massachusetts Avenue, Cambridge, Massachusetts 02139 USA

Abstract

Electrically triggered drug delivery represents an attractive option for actively and remotely controlling the release of a therapeutic from an implantable device (e.g., a “pharmacy-on-a-chip”). Here we report the fabrication of nanoscale thin films that can release precise quantities of a small molecule drug in response to application of a small, anodic electric potential of at least +0.5 V versus Ag/AgCl. Films containing negatively charged Prussian Blue (PB) nanoparticles and positively charged gentamicin, a small hydrophilic antibiotic, were fabricated using layer-by-layer (LbL) assembly. When oxidized, the PB nanoparticles shift from negatively charged to neutral, inducing dissolution of the film. Films with thicknesses in the range 100–500 nm corresponding to drug loadings of 1–4 μg/cm^2 were characterized. We demonstrate control over the drug dosage by tuning the film thickness as well as the magnitude of the applied voltage. Drug release kinetics ranging from triggered burst release to on/off, or pulsatile release, were achieved by applying different electric potential profiles. Finally, the *in vitro* efficacy of the released drug was confirmed against *Staphylococcus aureus* bacteria. Given the versatility of an external electrical stimulus and the ability of LbL assembly to conformally coat a variety of substrates regardless of size, shape, or chemical composition, we maintain that electrically controlled release of a drug from an LbL-coated surface could have applications in both implantable medical devices and transdermal drug delivery systems.

Keywords

layer-by-layer assembly; polymer thin film; drug delivery; electrochemistry; responsive materials; Prussian Blue

Introduction

Recently, there has been a growing interest in the development of “smart” devices capable of actively controlling the release of therapeutics *in vivo* in response to external stimuli in order to address a number of clinical needs.[1, 2] In particular, electronically-mediated drug delivery has seen a surge of interest owing to the precise control possible with an electric stimulus.[3–9] In comparison with other stimuli such as changes in pH, ionic strength,

CORRESPONDING AUTHOR FOOTNOTE. Tel: +1 617 258 7577. Fax +1 617 258 5766. hammond@mit.edu (P.T. Hammond).

Supporting Information Available: AFM height and phase images of the ITO-coated glass substrate with and without the $(PB/Chi)_5$ base layers, AFM height and phase images of a $Chi(PB/Chi)_5(PB/GS)_{75}$ film, cyclic voltammograms of a $Chi(PB/Chi)_5(PB/GS)_{25}$ film with increasing scan rate, confirmation of full PB electroactivity, chronocoulometry plots at each voltage investigated, further details on drug release kinetics modeling, AFM height images of $Chi(PB/Chi)_5(PB/GS)_n$ films throughout the dissolution process, and a comparison of PB oxidation kinetics and drug release kinetics are included. This material is available free of charge via the Internet at http://pubs.acs.org.

temperature, exposure to light, or application of a magnetic field, an electrical stimulus can be applied rapidly, remotely, reversibly, and locally (at an electrode surface instead of throughout the bulk), while maintaining mild conditions amenable to biological systems. These advantages make possible a host of drug release profiles ranging from sustained to pulsatile release in a pre-programmed manner or in real-time response to physiological changes. Furthermore, advances in microelectromechanical systems (MEMS) technology make possible future implantable devices that could integrate both biosensing and drug delivery components in a self-contained "pharmacy-on-a-chip".[10–12]

A critical component of every drug delivery system is the matrix or reservoir that contains the drug molecules and controls their release. Layer-by-layer (LbL) thin films, which are fabricated by a surface-mediated self assembly process involving the alternate adsorption of materials with complementary charged or functional groups,[13] are a versatile platform for controlling the release of drugs from surfaces [14, 15] and are the constructs used in this work. LbL assembly provides nanoscale control over film composition and morphology and allows for the incorporation of multiple different functional or responsive components.[16, 17] Given these benefits, our group and others have previously explored LbL films for electrically controlled release of various molecules.[18–23] An important challenge toward the engineering of LbL-based drug delivery devices is specifically controlling the release of small molecule therapeutics, which comprise 85% of all FDA-approved drugs between 1981 and 2002.[24] Typically, for electrostatic-based LbL films, water solubility and polyvalency are requirements for direct inclusion into the films. To bypass this requirement and to expand the realm of candidate materials, scientists have reported a number of different strategies. For instance, in the case of small, uncharged, water-insoluble molecules, our group and others have utilized charged "carrier" species such as micelles[25–29] and cyclodextrins[30, 31] that possess a hydrophobic core to sequester the drug, and a charged, hydrophilic exterior for self-assembly into a film. Alternatively, some drugs can be covalently bound to charged carrier molecules in a so-called "pro-drug" approach,[32, 33] while others may be non-specifically absorbed into micro- and nanoporous LbL films from organic solutions.[34] For the case of some small, charged drugs and dyes, incorporation into LbL films can be done directly based on electrostatics. Previously, our group has shown that the multivalent, positively-charged, aminoglycoside antibiotic gentamicin can itself be loaded into a layer-by-layer film by electrostatics, and the release can be controlled utilizing a hydrolytically degradable polycation.[35, 36] Other small, positively-charged molecules may be complexed with polyanionic species prior to LbL deposition[37] or loaded into films after assembly through absorption and binding to free negatively charged sites in the film.[38] Similarly, many small, negatively-charged molecules may be complexed with polycationic species before film assembly[37, 39] or bound to free positively charged sites following film assembly.[40, 41]

Here we present the electrostimulated release of gentamicin sulfate (GS), a small molecule antibiotic, from an LbL assembled thin film coating composed of biocompatible materials. Gentamicin, which is widely used to treat and prevent infections associated with implanted devices, including orthopedic implants,[42] serves as the cationic component of the LbL film. It possesses up to five positively charged amines below its pKa (~8.2).[43] Nanoparticles of Prussian Blue (PB)—approved by the FDA in tablet form in 2003 and shown to have very low cytotoxicity in a previous publication from our group[23]—are the anionic component of the film. Chitosan (Chi), a biocompatible polycation derived from the shells of crustaceans, is used for the underlying adhesion layers only. To our knowledge, this is the first report of an LbL film composed primarily of nanoparticles and small molecules, and the first demonstration of systematic electro-activated drug release from such films. These films are assembled with the following architecture: $Chi(PB/Chi)_5(PB/GS)_n$, where *n* represents the number of deposited bilayers. Drug loading into the film is easily controlled by changing the

number of layers, while release of gentamicin can be precisely controlled with an electrochemical stimulus. Previously, our group has reported on the electrochemically-mediated dissolution of LbL films containing PB and polymer at an applied anodic potential.[23, 44] Electroactive PB nanoparticles, which are negatively charged in the film in the absence of an applied potential, can be switched to neutral at an anodic potential, leading to destabilization of the film. Unlike other works in the literature that rely upon changes in local pH induced by the hydrolysis of water,[18, 19, 21] this work uses smaller voltages that will not disrupt the local pH environment, thereby making this system milder and more amenable toward biomedical applications. Further, this work is the first report of electrically-triggered release of a *small molecule drug* from an LbL film and represents a generic platform for controlling the release of any multiply charged, small molecule drug that is not susceptible to degradation by application of a small (< 1.0 V) electric potential. We maintain that such platforms could ultimately be integrated with implantable or transdermal drug delivery devices to address unmet clinical needs.

Experimental Section

Materials

Chitosan (Chi, “medium molecular weight”, 75–85% deacetylated), iron(II) chloride tetrahydrate, potassium ferricyanide, potassium chloride (KCl), potassium hydrogen phthalate (KHPh), sodium chloride (NaCl), and acetic acid were purchased from Sigma Aldrich (St. Louis, MO). Gentamicin sulfate (GS), USP Grade was purchased from Teknova (Hollister, CA). ^{3}H-gentamicin sulfate (^{3}H-GS) (0.250 mCi total, 1 mCi/mL in ethanol, 0.200 mCi/g) was purchased from American Radiolabeled Chemicals (St. Louis, MO). Phosphate buffered saline (PBS), 1X was purchased from Mediatech (Manassas, VA). Hydrochloric acid and sodium hydroxide solutions for pH adjustments were purchased from VWR Scientific (Edison, NJ). Indium tin oxide (ITO)-coated glass slides (CD-50IN-CUV) were purchased from Delta Technologies, Limited (Stillwater, MN). *Staphylococcus aureus*, strain 25923 with no antibiotic resistance, was purchased from ATCC (Manassas, VA), and cation-adjusted Mueller Hinton Broth (CMHB) was purchased from BD (Franklin Lakes, NJ). All chemicals were used as received.

Preparation of polyelectrolyte solutions

Prussian Blue (PB) nanoparticle solutions were prepared as described previously.[44] The nanoparticles range in diameter from <1 nm to 15 nm, with a median diameter of 4–5 nm.[44] Gentamicin sulfate solutions were prepared at a concentration of 1 mg/mL containing 0.1 M sodium chloride (NaCl). Chitosan (Chi) was dissolved at a concentration of 1.5 mg/mL in 0.1 M acetic acid, stirred overnight, and then vacuum filtered through a polyethersulfone membrane with a pore size of 0.45 μm. Deionized water (18.2 MΩ-cm, Milli-Q Ultrapure Water System, Millipore) was used to prepare all solutions. The pH of all solutions was adjusted to 4.0 with HCl and NaOH.

Film assembly

ITO-coated glass slides were sonicated in a 4% solution of Micro-90 cleaning solution (Cole Parmer, Vernon Hills, IL) for 15 min, followed by two 15 min sonication cycles in deionized water. Next, the slides were dried with a stream of nitrogen and subjected to oxygen plasma for 5 min using a Harrick PDC-32G plasma cleaner on high RF power to remove any remaining organic contaminants and increase the negative charge density on the surface. The slides were then immediately immersed in a Chi solution for 1 hr and rinsed in three separate pH 4.0 water baths for a total of 3 min. The LbL assembly technique was employed through dip coating with an automated Zeiss HMS series programmable slide stainer. Films were constructed with the architecture $Chi(PB/Chi)_5(PB/GS)_n$, in which the

five (PB/Chi) bilayers served as an adhesion platform for the overlaying $(PB/GS)_n$ layers with n = 25, 50, or 75. Each individual layer was deposited by a 10 min immersion in the appropriate polyelectrolyte (Chi, PB, or GS) solution, followed by a cascade rinse cycle in three separate pH 4.0 water baths for a total of 3 min to remove weakly bound material. Following deposition, films were dried under a stream of nitrogen.

Film characterization

Film thicknesses were determined by profilometry (KLA Tencor P16 surface profiler) using a 2 mg tip force and a stylus with a 2 μm tip radius. Films were scored to the substrate surface with a razor blade and step heights were measured at five different locations. Surface morphology and roughness were characterized in the dry state via atomic force microscopy (AFM) using a Dimension 3100 Scanning Probe Microscope (Veeco Instruments, Plainview, NY) in tapping mode. PointProbe Plus AFM probes (Nanosensors, Neuchatel, Switzerland) with a nominal tip radius of less than 7 nm were used. Electrochemically triggered film deconstruction studies were carried out with a Princeton Applied Research EG&G 263A potentiostat/galvanostat in a three-electrode cell. The electrolyte was 15 mL of PBS, 1X at pH 7.4 to mimic physiological conditions. The working electrode was a conducting ITO-glass substrate (7 × 50 × 0.5 mm) coated with the polyelectrolyte thin film, the reference electrode was a Ag/AgCl (3M KCl) electrode (Cypress Systems, Chelmsford, MA), and the counter electrode was a Pt wire. Cyclic voltammetry (CV) and chronoamperometry (CA) were performed in either PBS or a deoxygenated 0.1 M KHPh electrolyte with the same electrodes.

Drug release characterization

To quantify the release of GS, films were assembled with a mixture of radiolabeled ^{3}H-GS and non-radiolabeled GS (1:600 by mass) through LbL assembly as described above. After film deposition, films were dried under a stream of nitrogen and then immersed in the PBS electrolyte solution at room temperature (~25 °C). Passive drug release is defined as release in the absence of an applied voltage (i.e., at the open circuit potential), whereas active drug release is in the presence of an applied voltage. During a drug release experiment, 1 mL aliquots were removed from the release bath at indicated time points and were analyzed for radioactive ^{3}H content through scintillation counting after the addition of 5 mL of ScintiSafe Plus 50% (Fisher Scientific, Atlanta, GA) with a Perkin Elmer Tri-Carb 2810 Liquid Scintillation Counter. Raw data (disintegrations per min per mL, DPM/mL) were converted to μg ^{3}H-GS/mL by using the conversion factor 2.2×10^6 DPM = 1.0 μCi = 5.0 μg ^{3}H-GS. Finally, the total amount of GS released from a single film was calculated according to the following equation:

$$M_i = C_i \times V_i + (1\ \text{mL}) \sum_{j=1}^{i-1} C_j (600)$$

where M_i (μg) is the total cumulative mass released from the film as of measurement i, C_i (μg/mL) is the concentration of sample i, V_i (mL) is the total volume of the film dissolution bath before measurement i, $(1\ \text{mL}) \sum_{j=1}^{i-1} C_j$ is the total mass in previously extracted samples, and 600 is equal to the mass ratio of total GS to ^{3}H-GS in the solution used for film assembly, which is assumed to be identical to the ratio in the film.

In vitro efficacy of released gentamicin

The *in vitro* efficacy of gentamicin released from the films was tested through a microdilution assay against *Staphylococcus aureus* bacteria following standard methods outlined by the Clinical and Laboratory Standards Institute (M26-A, 1999). The assay was performed in a 96-well plate with 150 μL of liquid culture per well comprising 135 μL of test medium (i.e., PBS containing gentamicin released from an $n = 75$ film (see below), or PBS only for the positive control) and 15 μL of inoculation culture at 10^6 CFU/mL in cation-adjusted Mueller Hinton Broth II (CMHB). All test media were sterile-filtered through 0.2 μm cellulose acetate membranes immediately prior to use. Gentamicin was released from a 75 bilayer film exposed to +1.25 V (vs. Ag/AgCl) for 1 hr in 5 mL of PBS, yielding a gentamicin concentration of approximately 4.0 μg/mL. This maximum strength medium was serially diluted into an equal quantity of CMHB eight times in the 96-well plate, yielding a total of nine concentrations down to 0.016 μg/mL. A negative control in the absence of inoculated bacteria, and a positive control in the absence of gentamicin were included in the assay. All samples were measured in triplicate. The plate was incubated at 37 °C for 16 hr. Relative bacterial cell density was determined by recording the optical density (OD) at 600 nm in a BioTek PowerWave XS Microplate spectrophotometer with accompanying Gen5 software.

Results and Discussion

Film Growth and Surface Morphology

The thickness of the $Chi(PB/Chi)_5(PB/GS)_n$ films was monitored with profilometry (Fig. 1). The films were observed to assemble with super-linear growth behavior in contrast to previously reported LbL films containing PB nanoparticles.[44] This growth behavior is common for species that can interdiffuse through the multilayer film instead of depositing only as a single molecular layer on the film surface.[45] Gentamicin-containing LbL films reported previously by our group also showed super-linear growth behavior.[35] Indeed, it is not surprising that gentamicin, a small molecule with MW 477 g/mol, can diffuse within the film during assembly. An additional potential source of the super-linear growth behavior is the increased surface roughness of the film,[46] and thus increased surface area for adsorption with the deposition of additional layers (refer to text below on AFM studies).

An important factor critical to the growth of the films is the use of underlying adhesion or base multilayers. Interestingly, the initial deposition of five (PB/Chi) adhesion layers, while only ~24 nm thick, had a substantial effect on overall film growth (i.e., the thickness per deposited bilayer). As seen in Figure 1, $Chi(PB/GS)_n$ films (i.e., without adhesion layers) are ultrathin with a bilayer thickness of less than 1 nm,[47] while $Chi(PB/Chi)_5(PB/GS)_n$ films grow with bilayer thicknesses ranging from 3.4–5.6 nm. In the absence of the adhesion layers, it is possible that the pentavalent gentamicin is unable to adhere to the substrate in sufficient quantities to reverse the surface charge due to its limited cooperative binding ability compared to a flexible polyelectrolyte. Similarly, the low surface roughness of the substrate without adhesion layers may result in an insufficient number of available adsorption sites. The RMS roughness values, as calculated from AFM height images of films in the dry state (Fig. S1 in the Supporting Information), are 2.4 ± 0.2 nm and 4.4 ± 0.4 nm for the bare ITO substrate and the $Chi(PB/Chi)_5$ adhesion layers, respectively. Since the difference in surface roughness is not substantial, it seems more likely that the adhesion layers permit interlayer diffusion of gentamicin in sufficient quantities such that it can more easily reverse the surface charge. Since gentamicin and chitosan are both carbohydrates, and thus chemically similar, there is reason to believe that the chitosan-containing adhesion layers could serve as a reservoir for the absorption of gentamicin.

The surface morphology and roughness of the Chi(PB/Chi)$_5$(PB/GS)$_n$ films in the dry state were investigated with AFM and optical microscopy (Fig. 2). The RMS roughness of each film surface, as calculated from AFM height images, was 8.9 ± 0.5 nm, 11.2 ± 0.4 nm, and 35.7 ± 1.8 nm for n = 25, 50, and 75, respectively. Accordingly, we observed larger features on the film surface for an increasing number of deposited bilayers. Optical microscopy allows visualization of these features for the n = 75 film; however, the n = 25 and 50 films are featureless when viewed with this microscope due to insufficient resolution. It is likely that these features are regions of clustered Prussian Blue nanoparticles; similar nanoparticle clustering has been observed in other layer-by-layer systems.[48] Analysis of the AFM height and phase images over the same scan area (Fig. S2 in the Supporting Information) shows a greater phase angle in the regions containing the clusters. Since phase imaging provides contrast with respect to material mechanical properties, this observation supports the hypothesis that the cluster regions consist primarily of one of the film components, most likely the PB nanoparticles. Besides the presence of clusters, the optical micrograph also shows microscale cracks in the n = 75 film that have developed due to internal film stresses during drying.

Electrochemical Analysis

The electrochemical behavior of Chi(PB/Chi)$_5$(PB/GS)$_n$ films was investigated with cyclic voltammetry and chronocoulometry. Cyclic voltammetry over the potential range −0.4 V to 1.25 V (vs. Ag/AgCl) in PBS at a scan rate of 50 mV/s shows the full range of Prussian Blue redox states (Fig. 3). The fully reduced state is known as Prussian White (PW) ($Fe^{II}[Fe^{II}(CN)_6]^{2-}$), the mixed valence state is known as Prussian Blue (PB) ($Fe^{III}[Fe^{II}(CN)_6]^{1-}$), and the fully oxidized state is known as Prussian Yellow or Prussian Brown (PX) ($Fe^{III}[Fe^{III}(CN)_6]^{0}$) with a partially oxidized Berlin Green state. The half-peak potentials observed here are $E_{1/2,\ PW\text{-}PB}$ = 0.018 V and $E_{1/2,\ PB\text{-}PX}$ = 0.81 V both versus a Ag/AgCl (3M KCl) reference electrode. These values are shifted to slightly lower values than those reported for inorganic PB films[49] as well as other PB-containing LbL films.[44] As noted previously by our group,[44] this observation is consistent with the fact that a multivalent counterion in place of potassium, in this case gentamicin, is balancing the charge on the PB exterior sites; similar results have been observed elsewhere.[50] Upon multiple CV scans over the entire voltage range, the peak heights (and peak areas) continually decrease indicating a loss of Prussian Blue from the film (Fig. 3). When switching between the PB and PW states only, the voltammograms for multiple scans overlap exactly (data not shown) indicating no loss of material. Thus, as reported previously by our group,[23, 44] switching to the fully oxidized PX state leads to dissolution of the film. Refer to Fig. S3–S5 in the Supporting Information for additional details on electrochemical switching kinetics and confirmation that all of the PB nanoparticles in the film are electrochemically accessible.

Electrodissolution and Drug Release

The electrochemically triggered dissolution of Chi(PB/Chi)$_5$(PB/GS)$_n$ films was investigated by applying an electric potential for different periods of time in PBS buffer and then measuring the resulting film thickness with profilometry (Fig. 4). When a potential sufficient to oxidize the PB nanoparticles is applied to the film-coated electrode, electrons flow through the percolative network of nanoparticles in the film as they are removed from the Fe^{II} atoms and transferred to the electrode and then through the external circuit. The result of this process is a change in the net charge of the particles from negative to neutral. The ionic crosslinks binding the PB to the positively charged gentamicin are thus broken, and there is now an excess of positive charge present in the film. To maintain electroneutrality in the film, anions from solution and water (from both solvation of the anions and electroosmotic flux) will enter the film and solubilize the formerly bound gentamicin. The film will then dissolve as gentamicin is solubilized and diffuses into the

solution, along with some of the neutralized PB nanoparticles. Application of +1.25 V (vs. Ag/AgCl) induces a clear loss of material from the film. Soaking the films in the PBS buffer for 1 hr with no applied potential, however, does result in some loss of material from the film (an $n = 50$ film decreased in thickness by roughly 9%). Refer to the text below for further discussion on passive dissolution and drug release. During application of a potential, no delamination of the film is observed at the electrode and no precipitates are observed in the release bath; instead, the components of the film are released into the PBS as soluble molecules and/or complexes. As expected, the thicker films deconstruct more slowly than the thinner films due to the increased diffusion time required for both percolation of charge/current through the film and access of the film components to the surrounding aqueous solution to achieve a given degree of dissolution. The time to 50% dissolution (considering only the dissolvable portion of the film within 60 min) is roughly 1 min 11 sec, 1 min 57 sec, and 10 min 40 sec for the 25, 50, and 75 bilayer films, respectively; the corresponding film thicknesses of these films were 85.3 ± 9.0 nm, 181.0 ± 23.5 nm, and 519.1 ± 54.0 nm. Interestingly, the films are not completely removed from the substrate; instead the thicknesses plateau to approximately 25–45% of the initial film thicknesses. Likely, a portion of the neutral Prussian Yellow nanoparticles, which would not be expected to be readily solubilized or stable as a suspension in the aqueous electrolyte, aggregates irreversibly on the substrate surface along with an amount of trapped drug. The amount of drug released from an $n = 75$ film at +1.25 V for one hour, as discussed below, was compared to the total amount of drug in the film by dissolving an identical film in 0.01 M NaOH, which rapidly dissolves the Prussian Blue nanoparticles to their constituent iron salts. It was found that approximately 88% of the total drug in the film is released by application of the voltage. Therefore, the material remaining on the substrate must consist primarily of oxidized PB, chitosan, and roughly 12% of the initial amount of encapsulated drug.

The total drug loading into the film and drug release kinetics were studied as a function of the number of deposited layers. Films with architecture $Chi(PB/Chi)_5(PB/^3H\text{-}GS)_n$ were assembled with radioactively labeled drug (^{3}H-GS) (see Materials & Methods section), and the amount of drug released in PBS buffer over a duration of 60 min was measured via scintillation counting. Fig. 5A shows the release of gentamicin from $n = 25$, 50, and 75 bilayer films at a constant applied voltage of +1.25 V (vs. Ag/AgCl) over 60 minutes, demonstrating that the dosage size can be precisely controlled simply by adjusting the number of deposited layers. At the open circuit potential (OCP), which was roughly +0.25 V, a non-negligible amount of drug is released, equating to roughly 10–15% of the total releasable amount of drug in 60 min. Conceivably, this passive drug release is a combination of drug molecules that are weakly bound to the film plus drug molecules that are released from the partial dissolution of the film as mentioned above. While the passive release appears to plateau, drug release studies over a much longer duration reveal that approximately 67% of the total releasable drug in the film (from an $n = 75$ film) is released after 1 month in PBS. Thickness measurements confirm (data not shown) that the film thickness decreases substantially over this time frame as well. We suspect that the chemical instability of the Prussian Blue at high pH[51] is responsible for the dissolution of these films in the absence of an applied potential. Nonetheless, we are able to precisely control drug release actively in short to moderate timeframes relevant to a range of applications by applying an electric potential.

The active drug release kinetics were well fit by an empirical pseudo-second order model of the form shown in Eqn. 1, which was adapted from Ho et al. (Fig. 5B).[52] As was also done by Ho et al., we attempted to fit the experimental data to a pseudo-first order model and a diffusion-based model; however, these fits were poor (not shown). See the Supporting Information for further discussion. In the

$$\frac{dM(t)}{dt} = k(M_\infty - M(t))^2 \quad (1)$$

pseudo-second order model that we used, *M(t)* is the total cumulative mass of gentamicin released at time, *t*, M_∞ is the total mass of all releasable drug, and *k* is a second order rate constant. After integrating from time 0 to time t, the Eqn. 2 results. Therefore, a plot of *t*/*M*(*t*) versus *t* should be linear

$$\frac{t}{M(t)} = \frac{1}{kM_\infty{}^2} + \frac{1}{M_\infty}t \quad (2)$$

with slope $1/M_\infty$ and intercept $1/(kM_\infty)$. The second order rate constants for drug release rate (normalized to the total amount of drug released from each film) were determined to be $0.77 \pm 0.18\ min^{-1}$, $0.70 \pm 0.12\ min^{-1}$, and $0.58 \pm 0.05\ min^{-1}$, for the *n* = 25, 50, and 75 films, respectively. While the number of deposited bilayers has a significant impact on the kinetics of film dissolution versus time at +1.25 V (Fig. 4), the corresponding time scales of drug release (Fig. 5) are much more comparable. Specifically, the time to 50% drug release is roughly 57 sec, 1 min 17 sec, and 1 min 34 sec for the *n* = 25, 50, and 75 films, respectively. The time scales of drug release and film erosion match up relatively well for the *n* = 25 (1 min 11 sec for erosion, 57 sec for drug release) and *n* = 50 films (1 min 57 sec for erosion, 1 min 17 sec for drug release); however, there is a greater discrepancy between those values for the *n* = 75 film (10 min 40 sec for erosion, 1 min 34 sec for drug release). We hypothesize that the difference between the rate of thickness decrease and drug release is indicative of a surface erosion mechanism in which a non-uniform distribution of drug exists within the films (i.e., a higher concentration of drug toward the top of the film, which is expected for the diffusing component in exponentially growing layer-by-layer systems). A model for exponentially growing LbL films was proposed by Lavalle et al.[53] and Picart et al.,[45] in which the diffusing component diffuses throughout the entire film during deposition of that component; then when the film is exposed to the non-diffusing polyelectrolyte solution, the diffusing component will migrate to the outermost regions of the film for charge compensation with the newly deposited material. That hypothesis in itself could justify how films could develop a non-uniform distribution of components. Beyond that work, Porcel et al. later showed direct experimental evidence (utilizing confocal laser scanning micrscopy and fluorescently labeled polyelectrolytes) of films enriched toward the outermost portion of the film in the diffusing component,[54] which agreed with zone models proposed by Hubsch et al.[55] and Salomaki et al.,[56] who suggested there exists a “forbidden” zone a certain depth into the film into which a diffusing species cannot readily penetrate. Relatedly, our group previously compared the controlled release of heparin, an interdiffusing polyanion, with dextran sulfate, a non-diffusing polyanion, from hydrolytically degradable thin films.[57, 58] For these linearly surface eroding systems, it was found that the release rate of heparin was faster than the rate of film erosion, suggesting that an outer zone of the film is enriched in the diffusing species.[57, 58] AFM surface studies on $Chi(PB/Chi)_5(PB/GS)_n$ films electrochemically dissolved at +1.25 V over time reveal that the surface roughness remains the same or even decreases (Fig. S6 in the Supporting Information), as opposed to the formation of pits and furrows within the film that would be expected for bulk erosion. This observation suggests that the films do indeed dissolve by a surface erosion mechanism.[59, 60]

Next, the drug release behavior from films at different applied voltages was studied to examine the impact of voltage on the dose (Fig. 6) (Table S2 in the Supporting Information). In the absence of an applied potential (at the open circuit potential, +0.25 V), approximately 10–15% of the drug is released from the film over 1 hour, which was the standard drug release duration used in this study. Upon application of +1.25 V, there is a marked increase in the release rate of the drug as the Prussian Blue is fully oxidized to its neutral state. Application of +1.00 V is also sufficient to fully oxidize PB since this voltage is higher than the measured half-peak potential of +0.81 V. The amount of drug released at +1.25 V after 60 minutes appears greater than that released at +1.00 V; however, the means are not statistically different ($p = 0.15$). At +1.25 V, hydrolysis of water occurs at the electrode interface as evidenced by the fact that the charge removed from the film does not plateau with time (see Fig. S5 in the Supporting Information). At +1.00 V, however, the charge does plateau, indicating little to no hydrolysis is occurring; this result further confirms that oxidation of Prussian Blue, and not hydrolysis of water, is the primary mechanism responsible for film dissolution. The application of +0.75 V or +0.50 V also destabilizes the film and results in release of drug. These potentials are below the half-peak potential exhibited by the films, such that not all of the PB in the film will be oxidized and less of the drug will be released. Given the extremely broad peaks in the CV (Fig. 3), we hypothesize that non-equivalent electrochemical sites exist within the film due to differences in ionic binding or complexation within the matrix, which are more easily oxidized at these lower potentials, resulting in only partial destabilization of the film. We also observe that the kinetics of charge removal from the film, measured via chronocoulametry, match up well with the kinetics of drug release at +0.50 V to +1.00 V (see Fig. S7 in the Supporting Information).

Electrochemically reducing the PB in the film, on reversal of the current, partially at 0 V or fully at −0.25 V, results in the release of a statistically greater amount of drug than at the open circuit potential. As shown in a previous publication by our group, reducing PB in a polymer/nanoparticle LbL film doubles the charge on the PB surface and interior, resulting in film swelling.[61] It is possible that the charge imbalance created in the film upon reduction of PB induces partial release of the encapsulated drug. Alternatively, it is known that PB in its reduced state can electrocatalyze the reduction of dissolved oxygen,[62] which can increase the local pH environment. Since PB becomes chemically unstable at elevated pH levels,[51] partial dissolution of the film may also be occurring through this mechanism. Further studies on the mechanism of drug release upon electrochemical reduction of PB are beyond the scope of this paper.

Besides application of a constant potential, the drug release behavior under the influence of short electric potential pulses was investigated. While the results discussed above involved application of a constant potential for one hour, shorter pulse lengths at +1.25 V allow release of smaller doses of drug (Table 1). The fact that significant amounts of drug can be released with short pulses is important for device applications because shorter pulse lengths also require less power. Further, compared to the previously reported electrochemically controlled release of a model polymeric species (dextran sulfate) by Prussian Blue switching,[23] the drug in the films reported here is released more rapidly at the same applied voltage. We attribute this phenomenon to two possible factors: first, gentamicin is a small molecule with an expected higher diffusivity compared to a polymer; second, there is evidence that the top portion of the films is enriched in gentamicin due to its interdiffusing nature, whereas dextran sulfate is a non-diffusing species in LbL systems. In addition to applying a single short pulse, application of multiple short pulses of 2 seconds each allows the release of gentamicin to be turned on and off on demand for a pulsatile drug release profile (Fig. 7). The fact that the application of +1.25 V for only 2 seconds releases some drug, but does not permanently destabilize the film also suggests a surface erosion

mechanism; bulk erosion typically involves pitting and roughening of the surface,[59, 63] which would likely lead to an irreversible and rapid increase in the release rate of drug.

Efficacy of Released Drug

The *in vitro* efficacy of the gentamicin released from a $Chi(PB/Chi)_5(PB/GS)_{75}$ films against *S. aureus* bacteria was assessed using a microdilution assay. A potential of +1.25 V (vs. Ag/AgCl) was applied to a film in 5 mL of PBS, resulting in a concentration of approximately 4.5 μg/mL gentamicin. Serial microdilutions were made in a 96 well plate (see Methods) and cultured with *S. aureus* at a concentration of 10^5 CFU/mL for 16 h. Normalized bacterial cell density was calculated as $(OD_{600,sample} - OD_{600,negative\ control})/(OD_{600,\ positive\ control} - OD_{600,negative\ control})$. The minimum inhibitory concentration (MIC) exhibited by the gentamicin released from a $Chi(PB/Chi)_5(PB/GS)_{75}$ film was found to be in the range 0.25–0.50 μg/mL (Fig. 8). This value agrees well with the reported literature value of 0.25 μg/mL for the MIC of gentamicin against the same strain of *S. aureus*.[64] Thus, it is apparent that the gentamicin released from $Chi(PB/Chi)_5(PB/GS)_{75}$ films retains a comparable level of bactericidal activity compared to unmodified, commercial gentamicin. While application of an anodic potential can reportedly oxidize gentamicin in the presence of a metal electrocatalyst at very basic pH levels,[65] there is no evidence that this process occurs in the system reported here. Further, while it is known that gentamicin can form complexes with ferric and ferrous ions,[66] the existence of any such complexes and/or gentamicin-Prussian Blue complexes in the elution medium from the films reported here does not significantly affect the bactericidal activity of the drug.

Evaluation of the *in vivo* efficacy of gentamicin released from $Chi(PB/Chi)_5(PB/GS)_{75}$ films is beyond the scope of this study, but we can qualitatively assess whether the amount of drug released from our film would be sufficient to prevent or treat an infection based on studies from the literature. In a study by Darouiche et al., the authors simulated introduction of bacteria into a wound site during surgery by inoculating titanium alloy pins with 500 CFU of *S. aureus* (giving a maximum concentration of 2×10^4 CFU/mL at the wound site) and implanting them into rabbits.[67] They demonstrated that antimicrobial-coated implants had a significantly lower rate of colonization and thus were able to prevent infection. In a separate study by Alvarez et al., the authors established a bone infection in rabbits by introducing *S. aureus* bacteria into a drilled site in the femur at a concentration on the order of 10^8 CFU/mL.[68] After two weeks, the affected areas were cleaned, resulting in a bacteria concentration on the order of 10^4 CFU/mL, after which antibiotic-containing implants were inserted into the drill sites. They demonstrated that the implants were able to eliminate the bone infection within 3–4 weeks. Our results described above show that the amount of gentamicin released from a 75 bilayer film is sufficient to kill *S. aureus* bacteria at a concentration of 10^5 CFU/mL within 16 hr, an order of magnitude greater concentration than that present in the animal studies mentioned above. While the exact area and thickness of our films that would be used in an implant are not known, nor is the extent of dilution of the drug in the wound site over time, the results of our *in vitro* assay show that our films can release gentamicin in amounts sufficient to prevent and treat *S. aureus* infections.

Conclusions

In this paper, we have reported the fabrication and characterization of a nanoscale thin film that can release precise quantities of a small molecule drug in response to an applied electric potential. The films are fabricated by LbL assembly on the basis of electrostatic attraction between Prussian Blue nanoparticles and the small molecule antibiotic, gentamicin. Application of a voltage greater than *ca.* +0.50 V (vs. Ag/AgCl) destabilizes the film causing simultaneous release of the drug. We can control the drug loading into the film by tuning the number of deposited layers, and we can control the dose size and drug release

kinetics by applying different electric potential profiles. While slow release of drug does occur from the films in the absence of applied potentials, likely due to the inherent instability of PB at alkaline pH,[51] as reported by Ricci et al., many authors have developed PB-based biosensors for short-term use under physiological conditions, while others have been able to improve the pH stability of PB through various means.[51] Therefore, the system reported here could potentially be engineered for specific shorter-term medical applications, and/or different methods could be explored to enhance the pH-stability of the films.

In previous work, we controlled the release of a model polymeric species (dextran sulfate) from an LbL film with an applied electric potential.[23] Here we have improved upon that system by including an active therapeutic molecule and showing that the drug maintains its efficacy *in vitro*. Furthermore, the therapeutic is a small molecule drug, a class of materials that is difficult to incorporate into LbL films. In fact, this work is the first report of an LbL film comprised primarily of nanoparticles and small molecules, which could lead to interesting fundamental studies on the self-assembly principles of these materials. Since LbL assembly is such a simple and versatile process and can be used to coat substrates of any size or shape and can incorporate many different active pharmaceutical compounds, we believe that the system reported here is promising for controlling release autonomously or remotely in implantable or transdermal controlled drug release devices.

Supplementary Material

Refer to Web version on PubMed Central for supplementary material.

Acknowledgments

This work was supported primarily by the MRSEC Program of the National Science Foundation and made use of the MRSEC Shared Experimental Facilities under award number DMR – 0819762. It was also partially funded by the NIH National Institute of Aging and NIDCR via grant number 5R01AG029601-03. We thank the Center for Materials Science and Engineering (CMSE) and the Institute for Soldier Nanotechnologies (ISN) for access to experimental facilities, as well as Prof. Robert Langer for the use of the scintillation counter in his lab.

REFERENCES (Word Style “TF_References_Section”)

1. Kost J, Langer R. Adv Drug Delivery Rev 2001;46:125–148.
2. LaVan DA, McGuire T, Langer R. Nat Biotechnol 2003;21:1184–1191. [PubMed: 14520404]
3. Abidian MR, Kim DH, Martin DC. Adv Mater 2006;18:405–409.
4. Kulkarni RV, Biswanath S. J Appl Biomater Biomech 2007;5:125–139. [PubMed: 20799182]
5. Kwon IC, Bae YH, Kim SW. Nature 1991;354:291–293. [PubMed: 1956379]
6. Luo XL, Cui XT. Electrochem Commun 2009;11:402–404.
7. Murdan S. J Controlled Release 2003;92:1–17.
8. Pernaut JM, Reynolds JR. J Phys Chem B 2000;104:4080–4090.
9. Santini JT, Cima MJ, Langer R. Nature 1999;397:335–338. [PubMed: 9988626]
10. Grayson ACR, Shawgo RS, Li YW, Cima MJ. Adv Drug Delivery Rev 2004;56:173–184.
11. Razzacki SZ, Thwar PK, Yang M, Ugaz VM, Burns MA. Adv Drug Delivery Rev 2004;56:185–198.
12. Tsai HKA, Moschou EA, Daunert S, Madou M, Kulinsky L. Adv Mater 2009;21:656–660.
13. Decher G. Science 1997;277:1232–1237.
14. Lynn DM. Soft Matter 2006;2:269–273.
15. Lynn DM. Adv Mater 2007;19:4118–4130.
16. Bertrand P, Jonas A, Laschewsky A, Legras R. Macromol Rapid Commun 2000;21:319–348.
17. Hammond PT. Adv Mater 2004;16:1271–1293.
18. Boulmedais F, Tang CS, Keller B, Voros J. Adv Funct Mater 2006;16:63–70.

19. Dieguez L, Darwish N, Graf N, Voros J, Zambelli T. Soft Matter 2009;5:2415–2421.
20. Recksiedler CL, Deore BA, Freund MS. Langmuir 2006;22:2811–2815. [PubMed: 16519487]
21. Sato K, Kodama D, Naka Y, Anzai J. Biomacromolecules 2006;7:3302–3305. [PubMed: 17154455]
22. Wang F, Li D, Li GP, Liu XQ, Dong SJ. Biomacromolecules 2008;9:2645–2652. [PubMed: 18754640]
23. Wood KC, Zacharia NS, Schmidt DJ, Wrightman SN, Andaya BJ, Hammond PT. Proc Natl Acad Sci U S A 2008;105:2280–2285. [PubMed: 18272499]
24. Newman DJ, Cragg GM, Snader KM. J Nat Prod 2003;66:1022–1037. [PubMed: 12880330]
25. Addison T, Cayre OJ, Biggs S, Armes SP, York D. Langmuir 2008;24:13328–13333. [PubMed: 18954152]
26. Kim BS, Park SW, Hammond PT. ACS Nano 2008;2:386–392. [PubMed: 19206641]
27. Ma N, Zhang HY, Song B, Wang ZQ, Zhang X. Chem Mater 2005;17:5065–5069.
28. Manna U, Patil S. J Phys Chem B 2008;112:13258–13262. [PubMed: 18826302]
29. Nguyen PM, Zacharia NS, Verploegen E, Hammond PT. Chem Mater 2007;19:5524–5530.
30. Benkirane-Jessel N, Schwinte P, Falvey P, Darcy R, Haikel Y, Schaaf P, Voegel JC, Ogier J. Adv Funct Mater 2004;14:174–182.
31. Smith RC, Riollano M, Leung A, Hammond PT. Angew Chem, Int Ed 2009;48:8974–8977.
32. Kim BS, Lee H, Min YH, Poon Z, Hammond PT. Chem Commun (Cambridge, U K) 2009:4194–4196.
33. Thierry B, Kujawa P, Tkaczyk C, Winnik FM, Bilodeau L, Tabrizian M. J Am Chem Soc 2005;127:1626–1627. [PubMed: 15700982]
34. Berg MC, Zhai L, Cohen RE, Rubner MF. Biomacromolecules 2006;7:357–364. [PubMed: 16398536]
35. Chuang HF, Smith RC, Hammond PT. Biomacromolecules 2008;9:1660–1668. [PubMed: 18476743]
36. Moskowitz JS, Blaisse MR, Samuel RE, Hsu H-P, Harris MB, Martin SD, Lee JC, Spector M, Hammond PT. Biomaterials 2010;31:6019–6030. [PubMed: 20488534]
37. Chen H, Zeng GH, Wang ZQ, Zhang X. Macromolecules 2007;40:653–660.
38. Chung AJ, Rubner MF. Langmuir 2002;18:1176–1183.
39. Thierry B, Winnik FM, Merhi Y, Silver J, Tabrizian M. Biomacromolecules 2003;4:1564–1571. [PubMed: 14606881]
40. Kharlampieva E, Sukhishvili SA. Langmuir 2004;20:9677–9685. [PubMed: 15491202]
41. Wang L, Wang X, Xu MF, Chen DD, Sun JQ. Langmuir 2008;24:1902–1909. [PubMed: 18205423]
42. Schmidmaier G, Lucke M, Wildemann B, Haas NP, Raschke M. Injury 2006;37:105–112.
43. Newton DW, Kluza RB. Drug Intell Clin Pharm 1978;12:546–554.
44. DeLongchamp DM, Hammond PT. Adv Funct Mater 2004;14:224–232.
45. Picart C, Mutterer J, Richert L, Luo Y, Prestwich GD, Schaaf P, Voegel JC, Lavalle P. Proc Natl Acad Sci U S A 2002;99:12531–12535. [PubMed: 12237412]
46. Ruths J, Essler F, Decher G, Riegler H. Langmuir 2000;16:8871–8878.
47. The nanoparticle diameters range in size from <1 nm to 15 nm with a median diameter of 4–5 nm. It is possible to obtain multilayers with thickness of less than 1 nm per bilayer if the smallest nanoparticles are preferentially adsorbed or if submonolayer coverage of nanoparticles is achieved in each deposition step.
48. Zhang FX, Srinivasan MP. J Colloid Interface Sci 2008;319:450–456. [PubMed: 18155016]
49. Ellis D, Eckhoff M, Neff VD. J Phys Chem 1981;85:1225–1231.
50. Chen SM. J Electroanal Chem 2002;521:29–52.
51. Ricci F, Palleschi G. Biosens Bioelectron 2005;21:389–407. [PubMed: 16076428]
52. Ho YS, McKay G. J Environ Sci Health, Part A: Toxic/Hazard Subst Environ Eng 1999;34:1179–1204.

53. Lavalle P, Gergely C, Cuisinier FJG, Decher G, Schaaf P, Voegel JC, Picart C. Macromolecules 2002;35:4458–4465.
54. Porcel C, Lavalle P, Decher G, Senger B, Voegel JC, Schaaf P. Langmuir 2007;23:1898–1904. [PubMed: 17279672]
55. Hubsch E, Ball V, Senger B, Decher G, Voegel JC, Schaaf P. Langmuir 2004;20:1980–1985.
56. Salomaki M, Vinokurov IA, Kankare J. Langmuir 2005;21:11232–11240. [PubMed: 16285796]
57. Kim BS, Smith RC, Poon Z, Hammond PT. Langmuir 2009;25:14086–14092. [PubMed: 19630389]
58. Wood KC, Chuang HF, Batten RD, Lynn DM, Hammond PT. Proc Natl Acad Sci U S A 2006;103:10207–10212. [PubMed: 16801543]
59. Fredin NJ, Zhang JT, Lynn DM. Langmuir 2005;21:5803–5811. [PubMed: 15952826]
60. von Burkersroda F, Schedl L, Gopferich A. Biomaterials 2002;23:4221–4231. [PubMed: 12194525]
61. Schmidt DJ, Cebeci FC, Kalcioglu ZI, Wyman SG, Ortiz C, Van Vliet KJ, Hammond PT. ACS Nano 2009;3:2207–2216. [PubMed: 19624148]
62. Itaya K, Shoji N, Uchida I. J Am Chem Soc 1984;106:3423–3429.
63. Lu L, Garcia CA, Mikos AG. J Biomed Mater Res, Part A 1999;46:236–244.
64. Andrews JM. J Antimicrob Chemother 2001;48:5–16. [PubMed: 11420333]
65. Voegel PD, Baldwin RP. Electroanalysis 1997;9:1145–1151.
66. Priuska EM, Schacht J. Biochem Pharmacol 1995;50:1749–1752. [PubMed: 8615852]
67. Darouiche RO, Mansouri MD, Zakarevicz D, AlSharif A, Landon GC. J Bone Jt Surg (Am) 2007;89A:792–797.
68. Alvarez H, Castro C, Moujir L, Perera A, Delgado A, Soriano I, Evora C, Sanchez E. J Biomed Mater Res, Part B 2008;85B:93–104.

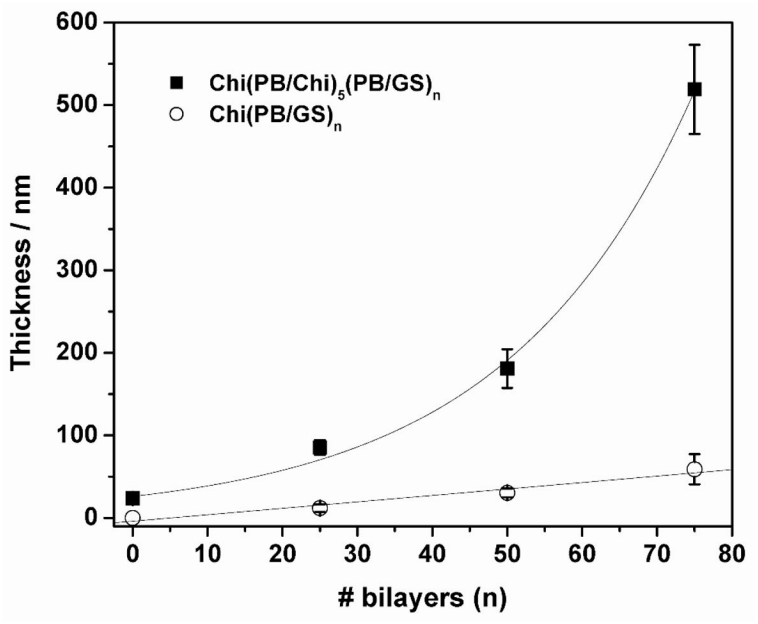

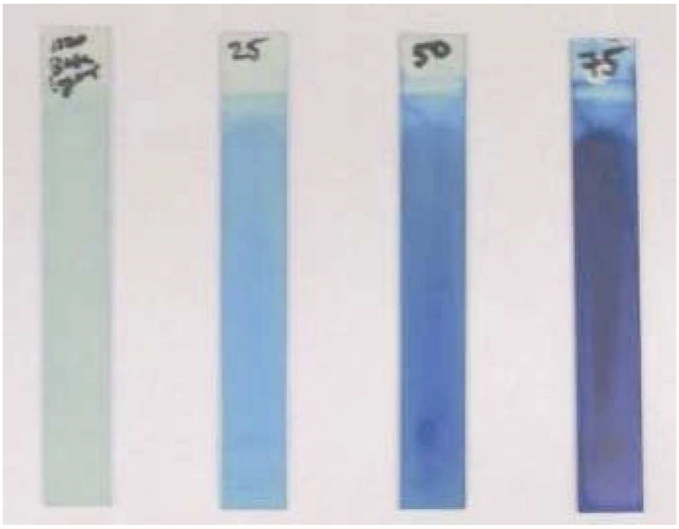

Figure 1.

A) Growth curve, determined via profilometry, for Chi(PB/Chi)$_5$(PB/GS)$_n$ and Chi(PB/Chi)$_n$ film architectures, revealing accelerated film growth when adhesion layers are deposited. The lines are best fit lines for exponential and linear growth models for films with and without adhesion layers, respectively. Error bars represent ± one standard deviation in measured thickness values at n = 5–7 locations on each film. B) Photographs of Chi(PB/Chi)$_5$(PB/GS)$_n$ films for n = 0, 25, 50, and 75.

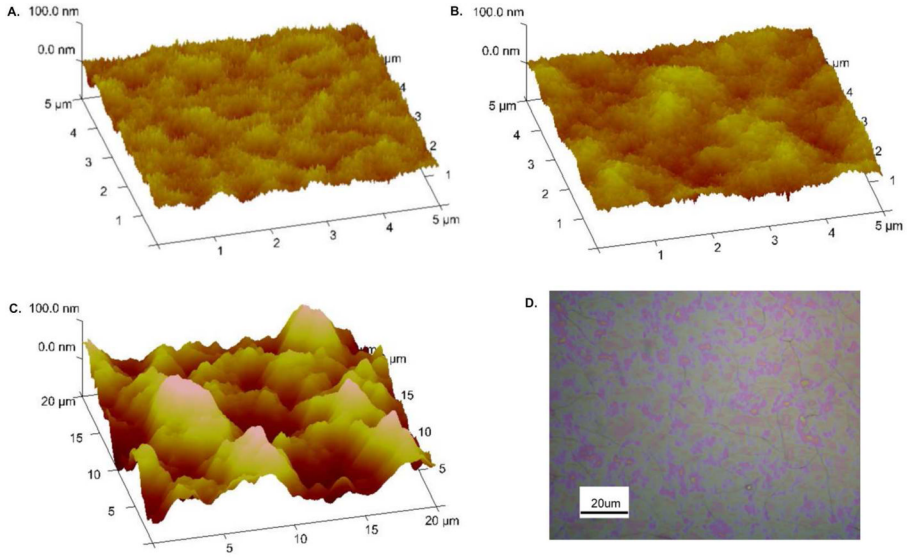

Figure 2.

Atomic force microscopy 3D height images of A) n = 25, B) n = 50, and C) n = 75 bilayer films and D) an optical micrograph of an n = 75 film. Film surface roughness increases and clusters form on the film surface with the deposition of an increasing number of bilayers.

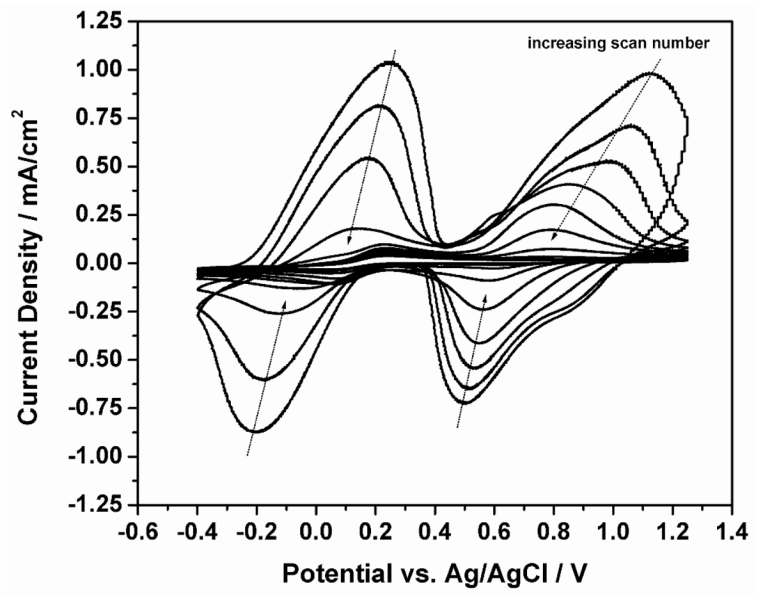

Figure 3.

Cyclic voltammograms of a Chi(PB/Chi)$_5$(PB/GS)$_{25}$ film subjected to multiple cycles at a scan rate of 50 mV/s in a PBS, pH 7.4 electrolyte. A decrease in peak height (and peak area) with subsequent scans reveals a loss of the electroactive Prussian Blue from the film.

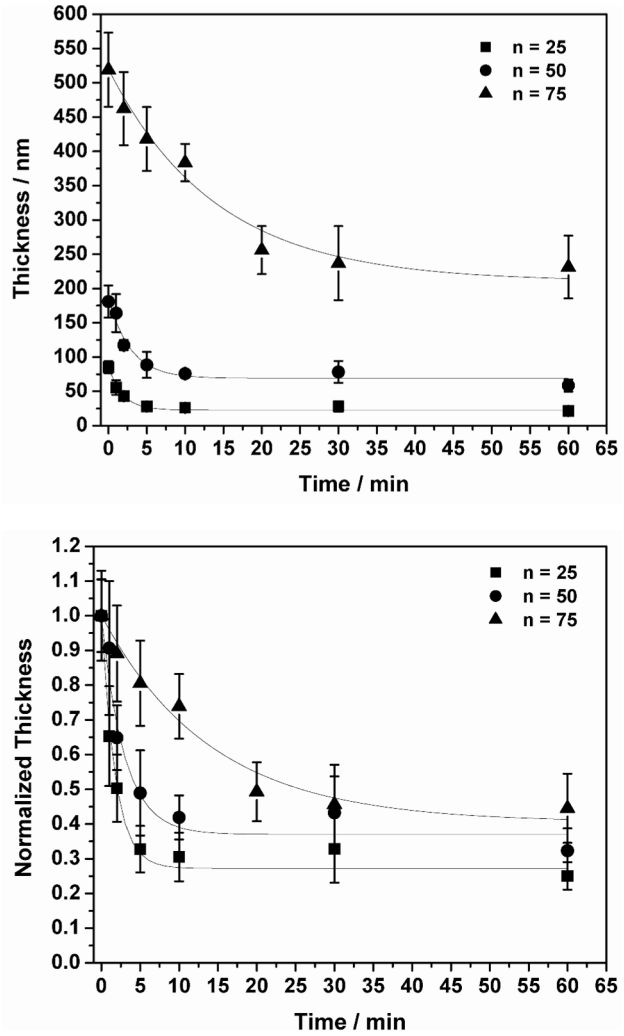

Figure 4.

A) Absolute and B) normalized thickness of Chi(PB/Chi)$_5$(PB/GS)$_n$ films over time at an applied potential of +1.25 V vs. Ag/AgCl in a PBS, pH 7.4 electrolyte. The thickest films dissolve more slowly, and all film thicknesses plateau to approximately 25–45% of initial thickness. The lines represent the best fit to a first order exponential decay model. Error bars represent ± one standard deviation in measured thickness values at n = 5–10 locations on each film.

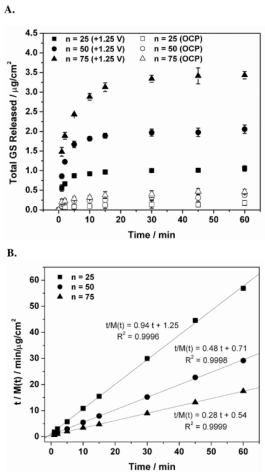

Figure 5.

(A) Drug release profiles from Chi(PB/Chi)$_5$(PB/GS)$_n$ films at an applied potential of +1.25 V vs. Ag/AgCl and at the open circuit potential (OCP). The total amount of released drug, or the drug dosage, can be set by tuning the number of deposited layers, *n*. Error bars represent ± one standard deviation in measured values from n = 3 films. (B) Linear regression best fits for a pseudo-second order drug release kinetics model for *n* = 25, 50, and 75 films.

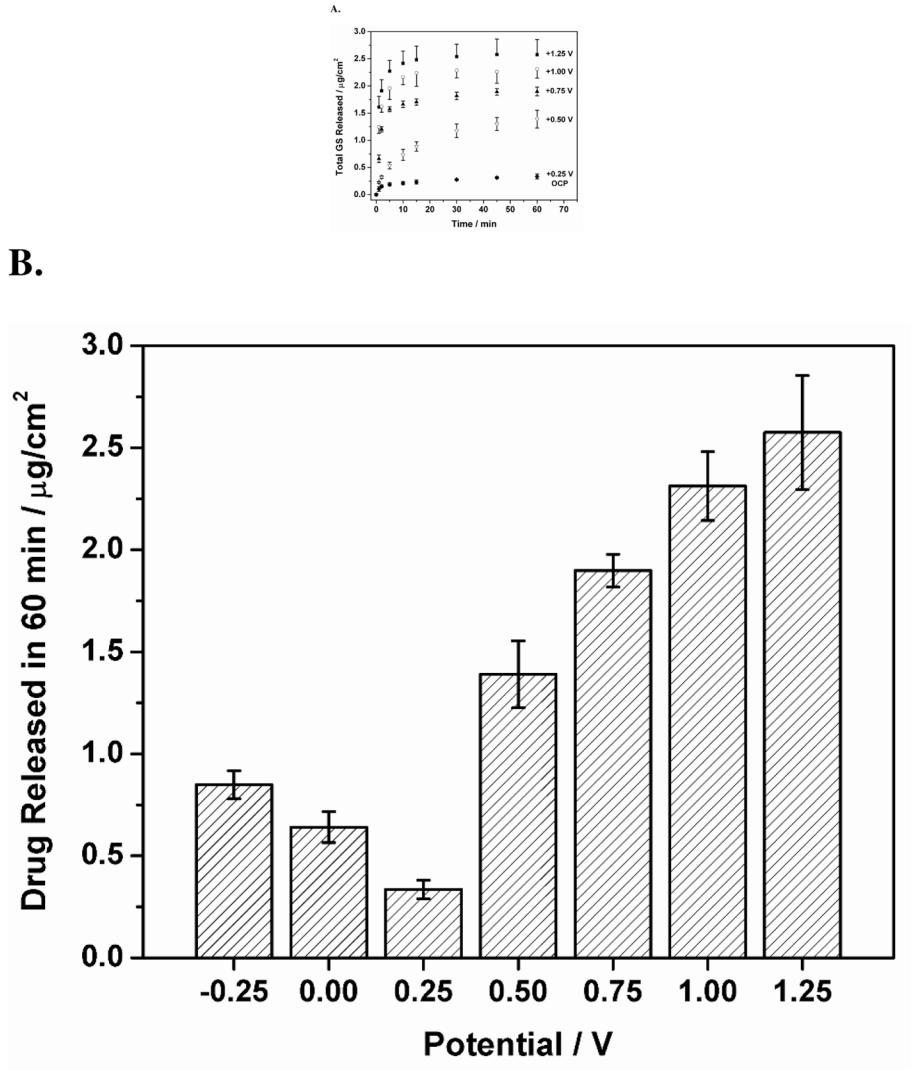

Figure 6.

A) Total amount of gentamicin released from a Chi(PB/Chi)$_5$(PB/GS)$_{50}$ film over time at different applied potentials. B) Total amount of gentamicin released from a Chi(PB/Chi)$_5$(PB/GS)$_{50}$ film in 1 hr at different applied potentials. The smallest amount of drug is released at the open circuit potential of +0.25 V, while increasing amounts of drug are released at both anodic and cathodic potentials, with the greatest amount released during oxidation of the PB. Error bars represent ± one standard deviation in measured values from n = 3 films. All means are statistically different from each other with $p < 0.05$ except for those at +1.00 and +1.25 V, for which $p = 0.15$.

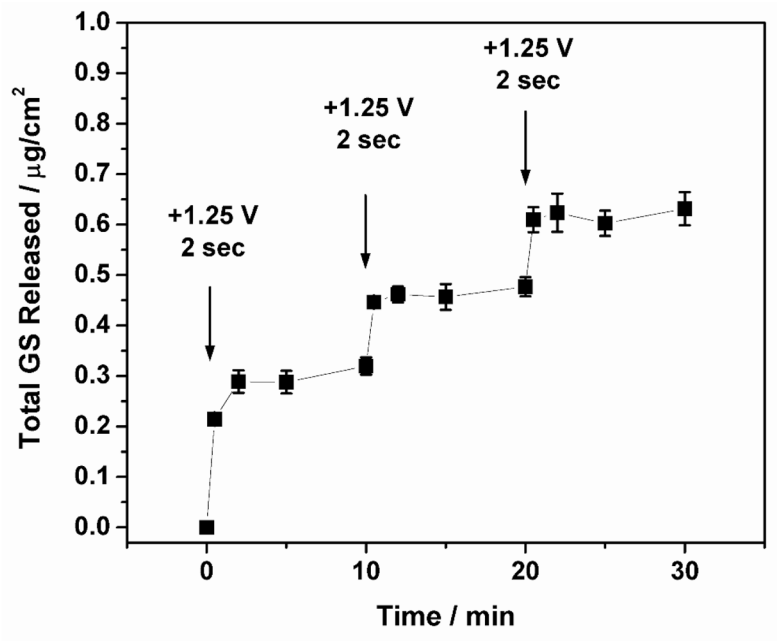

Figure 7.

Drug release profile from a Chi(PB/Chi)$_5$(PB/GS)$_{75}$ film with 2 sec pulses of +1.25 V to turn drug release 'on', followed by 30 sec pulses at +0.25 V to turn drug release 'off'. The films are sufficiently stable to allow for on/off, or pulsatile, drug release controlled by the applied potential. Error bars represent ± one standard deviation in measured values from n = 3 films.

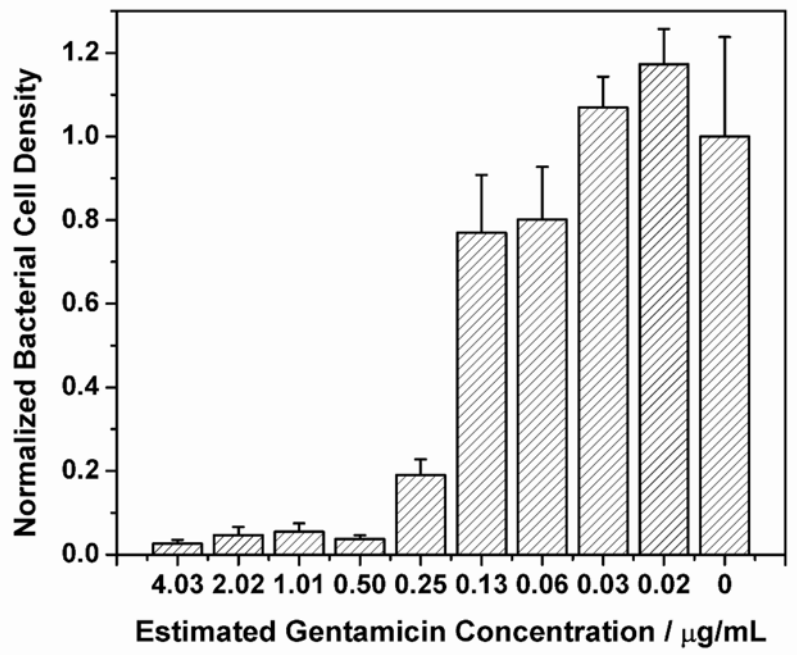

Figure 8.

Results of a microdilution assay of gentamicin released from a $Chi(PB/Chi)_5(PB/GS)_{75}$ film against *S. aureus* bacteria. The MIC of the drug released from the film corresponds well with that of the free drug. Error bars represent ± one standard deviation in measured values from n = 3 samples.

Table 1

The fraction of total gentamicin released from Chi(PB/Chi)$_5$(PB/GS)$_{50}$ films with different pulse lengths at +1.25 V vs. Ag/AgCl. The pulse length may be used to control the total amount of released drug. The standard deviations were determined from n = 3 films.

Pulse length at +1.25 V	Normalized Fraction of GS Released in 30 min[1]
0 sec	0.18 ± 0.02
2 sec	0.50 ± 0.04
5 sec	0.58 ± 0.11
30 sec	0.78 ± 0.03

[1] Drug release is normalized to the total amount of GS released in 30 min at a constant applied potential of +1.25 V.